Broadband optical frequency comb generation in lithium niobate microring resonator by dispersion engineering

Zhaolong Shi[1], Dongmei Huang[1,2*], Zihao Cheng[1,2], Feng Li[2], and P. K. A. Wai[2,3]
[1]*Photonics Research Institute, Department of Electrical and Electronic Engineering, The Hong Kong Polytechnic University, Hong Kong SAR, China*
[2]*The Hong Kong Polytechnic University Shenzhen Research Institute, Shenzhen 518057, China*
[3]*Department of Physics, Hong Kong Baptist University, Hong Kong, China*
*Corresponding author: meihk.huang@polyu.edu.hk

ABSTRACT

Thin film lithium niobate (LN) is considered a promising platform for integrated photonics owing to its exceptional electro-, nonlinear-, and acousto-optic properties. In this work, we propose the generation of broadband optical frequency combs in an LN microring resonator by dispersion engineering. We design the structure of the LN waveguide to adjust the effective refractive index of its fundamental mode so that the microring resonator can generate two dispersive waves near the pump light to achieve a broadband optical frequency comb up to 4/5-octave range (about 110 THz). The broadband frequency comb is crucial for future on-chip LN nonlinear photonics applications.

Keywords: Microring resonator, thin-film LN, frequency comb, dispersion engineering.

1. INTRODUCTION

Soliton Kerr optical frequency combs are widely used in optical measurements and spectroscopy[1]. A variety of material platforms including SiO_2[2] and AlN[3] have been proposed and demonstrated to generate optical frequency combs. Thin film LN with a wide transparency window, exceptional electro-, nonlinear-, and acousto-optic properties is a promising integrated optical material[4]. The nonlinear devices based on LN microcavities have attracted much interest. For most nonlinear applications such as optical frequency combs[5] and supercontinuum generation[6], the dispersion parameters significantly affect their performance. At present, several integrated optical frequency combs have been implemented on the LN platform, such as electro-optic frequency comb[7], LN Kerr optical frequency comb[8], and photorefractive effect assisted microresonator optical frequency comb[9]. The bandwidth generated by some devices however is still very narrow because of the lack of dispersion design.

In this paper, we propose a simple method for dispersion engineering in LN slab waveguide for broadband frequency comb generation. We analyze how the geometrical parameters affect the dispersion. Based on our results, we propose an LN microcavity design for broadband optical frequency comb generation. Through dispersion engineering, two dispersive waves (DW) can be used to broaden the optical frequency comb. Simulation results show that by adjusting structural parameters, such as waveguide thickness and width, the dispersive wave emission can be controlled and the bandwidth can be broadened to 4/5 octaves.

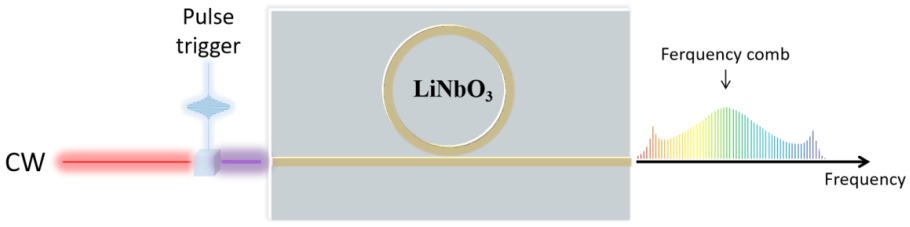

Fig. 1. Dissipative Kerr soliton generation in an LN microring resonator.

2. THEORETICAL MODEL

Different from the conventional tuning-based soliton generation approach, we propose a Kerr frequency comb generation scheme by the single pulse triggering. Fig. 1 illustrates the proposed scheme, where a continuous wave and the triggering pulse are combined and then injected into an LN microring resonator[10]. We use the Lugiato-Lefever equation (LLE) to model the evolution of the soliton in LN resonators. We include higher-order dispersion and self-steepening effects to calculate the propagation of the optical field in the microcavity[11]. The modified Lugiato-Lefever equation is given by,

$$t_R \frac{\partial E(t,\tau)}{\partial t} = \left[-\alpha - i\delta_0 + iL\sum_{n\geq 2} \frac{i^n \beta_n}{n!} \frac{\partial^n}{\partial \tau^n} + i\gamma L\left(1 + \frac{i}{\omega_0}\frac{\partial}{\partial \tau}\right) |E(t,\tau)|^2 \right] E(t,\tau) + \sqrt{\theta} E_{in}, \quad (1)$$

where $E(t,\tau)$ is the slowly varying envelope of the intracavity optical field, t_R is the roundtrip time, α is the roundtrip linear loss coefficient, δ_0 is the detuning between the CW pump frequency and the resonance frequency. θ is the coupling coefficient of the CW pump laser, and β_n represents the n-th order dispersion coefficient. γ is the self-phase modulation coefficient. L is the cavity length. E_{in} is the amplitude of the CW pump. The combined injected signal of a CW pump and a single shot pulse is given by[12],

$$E_{in-trigger} = E_{CW} + \sqrt{P_t}\exp(-i\Delta\Omega)\operatorname{sech}(\tau/\tau_t), \quad (2)$$

where E_{cw} is the CW pump field, and P_{t} and τ_{t} are the peak power and pulse width of the trigger pulse, respectively. $\Delta\Omega = 2\pi\Delta f = 2\pi(f_{\text{t}} - f_{\text{cw}})$ is the central frequency offset of the trigger with respect to the CW pump, where f_{t} and f_{cw} are the central frequencies of the trigger pulse and the CW field, respectively.

3. DISPERSION ENGINEERING

The design of the waveguide shape can effectively adjust its effective refractive index[13], here we choose a typical LN slab waveguide. The LN wafer is grown on a SiO_2 substrate, and the cladding is air. Fig. 2(a) shows the schematic cross section of the proposed LN waveguide where W is the waveguide width, θ is the sidewall angle, H is the waveguide height and h is the slab thickness. The exact frequency of the DW is determined by the waveguide geometry[14]. The broadband optical frequency comb generation depends on the engineering of the dispersion curve of the microring resonator. By varying the waveguide structure design, we can vary the dispersion curve of its modes for dispersive waves generation, which can broaden the optical frequency comb. The resonant frequency in the optical microcavity can be Taylor-expanded at the pump frequency ω_0,

$$\omega_\mu = \omega_0 + D_1\mu + \frac{D_2}{2!}\mu^2 + \frac{D_3}{3!}\mu^3 + \ldots = \omega_0 + D_1\mu + \sum_{n\geq 2}\frac{1}{n!}D_n\mu^n, \quad (3)$$

where, ω_μ is the resonant frequency of mode number μ, ω_0 is the pump frequency, and $D_1/2\pi$ is the FSR of the resonator. $D_2 = -cD_1^2\beta_2/n_0$ is related to the group velocity dispersion and D_{n}, n > 2, represents higher order dispersion coefficient. We introduced the integrated dispersion $D_{\text{int}}(\mu) = \omega_\mu - (\omega_0 + D_1\mu)$ to describe the deviation of the resonance frequency from the equidistant frequency grids[15]. Higher order dispersion determines the formation of dispersive waves for which the phase matching condition must be satisfied (i.e. $D_{\text{int}} = 0$) [16]. Fig. 2(b) shows that by dispersion engineering, dispersive waves are formed at both the blue and red sides of the pump frequency, which spans more than 100 THz. The location of the dispersive waves can be varied by adjusting D_{int}. In this paper, we focus on changing the integrated dispersion of the waveguide by varying its basic structural parameters.

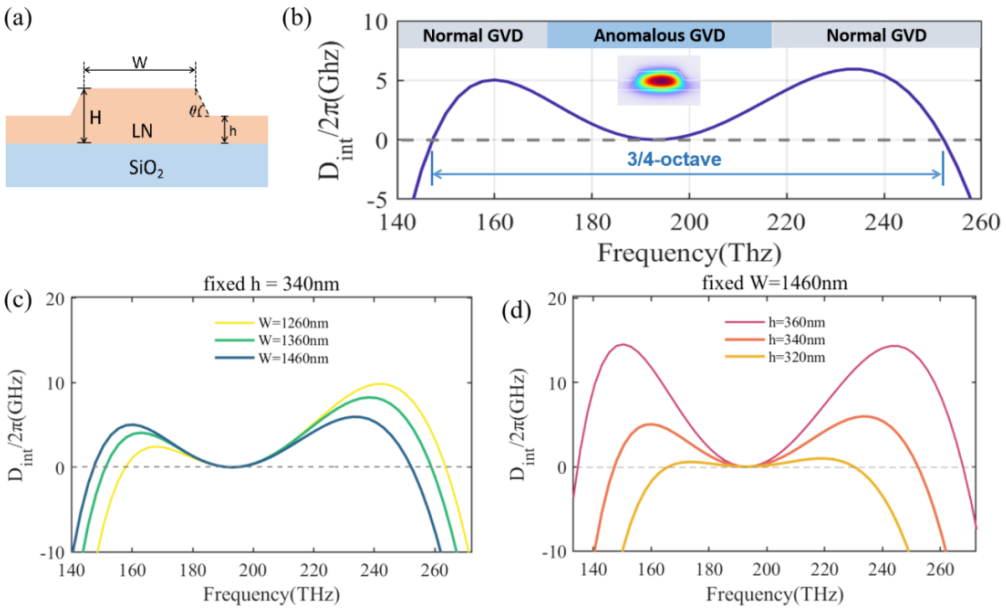

Fig. 2. (a) Schematic of the LN waveguide. Waveguide top width=W, Etch angle θ=60°, LN waveguide height H=620nm, and LN slab thickness=h; (b) Integrated dispersion (D_{int}) of the LN resonator with FSR=200 GHz. Simulated D_{int} curves as a function of frequency for different (c) W and (d) h.

We design a waveguide with an etch angle of 60° and a height of 620 nm, which can be fabricated by most processing equipment. We vary two waveguide parameters, the waveguide width (W) and the slab thickness (h), because they have more pronounced effect on the position of the dispersive wave. The radius of the microring resonator is 113 μm and the FSR = 200 GHz. We simulate the waveguide structure by the finite element method, and calculate the GVD and the higher-order dispersion coefficients. Fig. 2(c) shows that for a fixed waveguide height H and slab thickness h, smaller waveguide widths result in an overall blue shift of the spectrum. From Fig. 3(c), when the waveguide width decreases, the phase matching points of the two dispersive waves on the blue and red sides of the pump frequency are blue-shifted so that the separation between the two dispersive waves remains approximately the same. We also observe that when the waveguide width decreases, the maximum integrated dispersion of the DW on the blue side increases while that on the red side decreases. Fig. 2(d) shows that the slab thickness has a significant effect on the flatness of the integrated dispersion. A smaller h results in a flatter D_{int}, which results in a flatter comb teeth. However, the separation of the two dispersive waves decreases as h decreases, resulting in a decrease in the width of the frequency comb. For optimal performance, we choose the width and slab thickness to be W = 1460 nm and h = 340 nm, respectively.

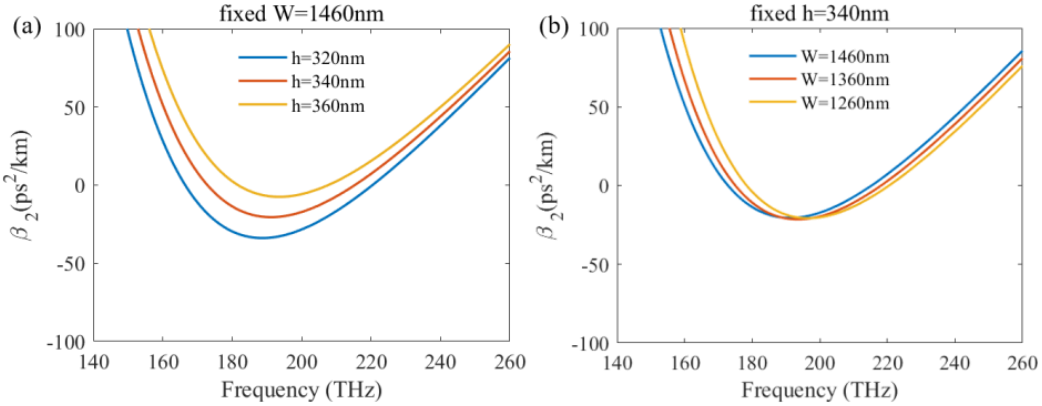

Fig. 3. Group velocity dispersion with different (a) h with W=1460 nm and (b) W with fixed h=340 nm. The etch angle θ=60°

In general, the effect of β_2 on the spectral shape of the optical frequency comb is more pronounced, and smaller GVD coefficients make it easier to realize a broadband optical frequency comb. Fig. 3(a) shows the variation of β_2 with frequency for different waveguide heights h when the waveguide width is 1460 nm. Fig. 3(b) shows the variation of β_2 with frequency for different waveguide widths W when the slab thickness is 340 nm. From Fig. 3, the slab thickness has greater influence on the GVD coefficient than the waveguide width. We note that when β_2 decreases, the two dispersive waves are closer together and thus the bandwidth of the frequency comb narrows.

4. SIMULATION RESULT

We have also studied the frequency comb evolution of an optical microcavity based on this waveguide design by using Eqs. (1)-(3). The simulation parameters are as follows: FSR = 200.0 GHz, α = 1.27 m^{-1}, γ = 0.86 $m^{-1}W^{-1}$, $\sqrt{\theta}$ = 41.45 m^{-1}, and $P_{in} = |E_{in}|^2$ = 0.07 W. The LN microcavity is pumped with a CW laser at a wavelength of 1550 nm, where the CW detuning was δ_0 = 0.0104. For the microring resonator, the second-, third-, and fourth-order dispersion coefficients are β_2 = −20.37 ps^2/km, β_3 = 0.0267 ps^3/km and β_4 = 0.00234 ps^4/km, respectively. A single-shot pulse trigger is used to generate the Kerr comb. The parameters of the trigger pulse are P_t = 10 kW, τ_t = 1.5 ps, and $\Delta\Omega = 2\pi \times 5 \times$FSR. Fig. 4(a) shows that multiple weak pulses emerge after the injection of the pulse trigger. The central pulse with the highest peak power gradually evolves into a soliton. Fig. 4(b) shows the evolution of the soliton spectrum. After about 5,000 roundtrips, the power inside the cavity stabilizes and forms a steady state with a single soliton as shown in Fig. 4 (c). Fig. 4(d) shows the spectrum of the stable single-soliton comb. There are two dispersive waves at frequencies of about 145 THz and 255 THz, consistent with the designed D_{int} curves shown in Fig. 2(c). The frequency comb spans close to 120 THz, which is more than 4/5 octave. The results show that the proposed structure can generate a broadband optical frequency comb.

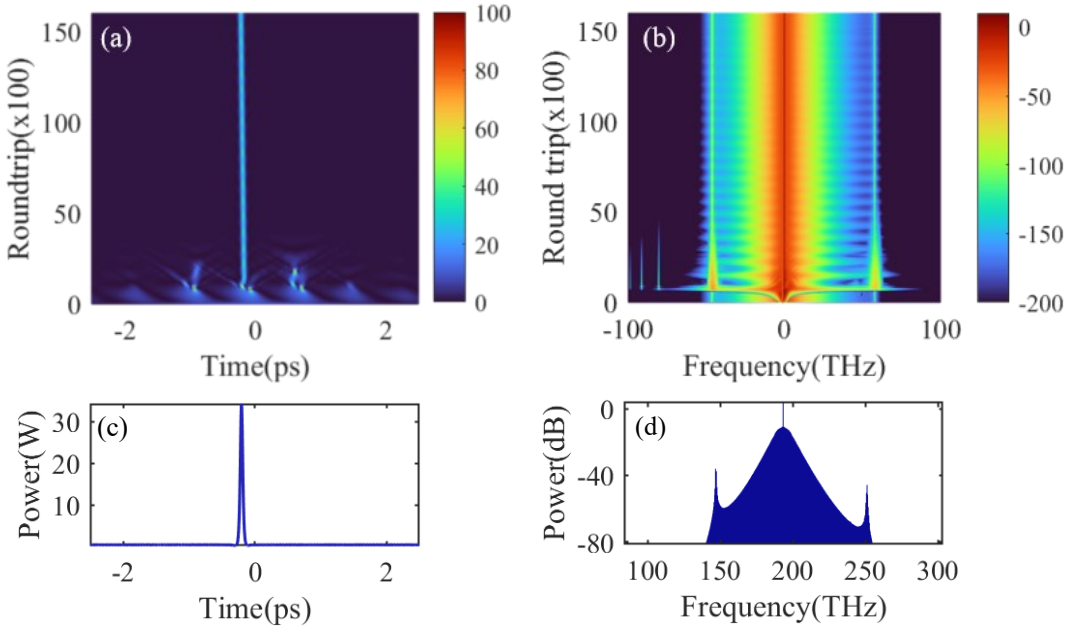

Fig. 4. Evolution of the (a) temporal waveform and (b) spectrum after the injection of the single pulse trigger. (c) Temporal waveform and (d) spectrum of the soliton frequency comb.

5. CONCLUSION

In conclusion, we present a monolithic integration scheme to generate broadband optical frequency combs spanning from the visible to the near-infrared wavelengths. We discuss how the top width of the microring resonator and the total thickness of the LN layer affect the dispersion curve. By optimizing these parameters, the desired dispersion curve can be achieved to generate broadband and stable single soliton frequency combs. Thus, the waveguide geometry can be used to engineer the dispersion of LN devices for frequency comb generation, and supercontinum generation, which can be used in applications such as spectroscopy, ranging, telecommunications and quantum processing[17–19].

ACKNOWLEDGEMENT

This research was supported in part by the National Key R&D Program of China (2020YFB1805901); in part by the National Natural Science Foundation of China (62105274); in part by supported by a grant from the Research Grants Council of the Hong Kong Special Administrative Region, China (PolyU15301022).

REFERENCES

[1] T. J. Kippenberg, A. L. Gaeta, M. Lipson, and M. L. Gorodetsky, "Dissipative Kerr solitons in optical microresonators," Science **361**(6402), eaan8083 (2018).

[2] X. Yi, Q.-F. Yang, K. Y. Yang, M.-G. Suh, and K. Vahala, "Soliton frequency comb at microwave rates in a high-Q silica microresonator," Optica **2**(12), 1078–1085 (2015).

[3] X. Liu, Z. Gong, A. W. Bruch, J. B. Surya, J. Lu, and H. X. Tang, "Aluminum nitride nanophotonics for beyond-octave soliton microcomb generation and self-referencing," Nat. Commun. **12**(1), 5428 (2021).

[4] J. Lin, F. Bo, Y. Cheng, and J. Xu, "Advances in on-chip photonic devices based on lithium niobate on insulator," Photonics Res. **8**(12), 1910–1936 (2020).

[5] P. Liu, H. Wen, L. Ren, L. Shi, and X. Zhang, "χ(2) nonlinear photonics in integrated microresonators," Front. Optoelectron. **16**(1), 18 (2023).

[6] F. Ye, J. Huang, and Q. Li, "Enhanced Dispersive Wave in the Dispersion Engineered Lithium Niobate Waveguides," in *26th Optoelectronics and Communications Conference* (Optica Publishing Group, 2021), p. T4E.6.

[7] R. Zhuang, K. Ni, G. Wu, T. Hao, L. Lu, Y. Li, and Q. Zhou, "Electro-Optic Frequency Combs: Theory, Characteristics, and Applications," Laser Photonics Rev. **17**(6), 2200353 (2023).

[8] C. Wang, M. Zhang, M. Yu, R. Zhu, H. Hu, and M. Loncar, "Monolithic lithium niobate photonic circuits for Kerr frequency comb generation and modulation," Nat. Commun. **10**(1), 978 (2019).

[9] Y. He, Q.-F. Yang, J. Ling, R. Luo, H. Liang, M. Li, B. Shen, H. Wang, K. Vahala, and Q. Lin, "Self-starting bi-chromatic $LiNbO_3$ soliton microcomb," Optica **6**(9), 1138–1144 (2019).

[10] Z. Cheng, F. Li, D. Huang, and P. K. A. Wai, "Deterministic single soliton excitation in LiNbO3 microcavity with fundamental-second-harmonic mode coupling," in *14th Pacific Rim Conference on Lasers and Electro-Optics (CLEO PR 2020)* (Optica Publishing Group, 2020), p. C4B_1.

[11] M. R. E. Lamont, Y. Okawachi, and A. L. Gaeta, "Route to stabilized ultrabroadband microresonator-based frequency combs," Opt. Lett. **38**(18), 3478 (2013).

[12] Z. Kang, F. Li, J. Yuan, K. Nakkeeran, J. N. Kutz, Q. Wu, C. Yu, and P. K. A. Wai, "Deterministic generation of single soliton Kerr frequency comb in microresonators by a single shot pulsed trigger," Opt. Express **26**(14), 18563 (2018).

[13] S. Fujii and T. Tanabe, "Dispersion engineering and measurement of whispering gallery mode microresonator for Kerr frequency comb generation," Nanophotonics **9**(5), 1087–1104 (2020).

[14] Z. Gong, X. Liu, Y. Xu, and H. X. Tang, "Near-octave lithium niobate soliton microcomb," Optica **7**(10), 1275 (2020).

[15] T. Herr, V. Brasch, J. D. Jost, C. Y. Wang, N. M. Kondratiev, M. L. Gorodetsky, and T. J. Kippenberg, "Temporal solitons in optical microresonators," Nat. Photonics **8**(2), 145–152 (2014).

[16] V. Brasch, M. Geiselmann, T. Herr, G. Lihachev, M. H. P. Pfeiffer, M. L. Gorodetsky, and T. J. Kippenberg, "Photonic chip–based optical frequency comb using soliton Cherenkov radiation," Science **351**(6271), 357–360 (2016).

[17] M. G. Vazimali and S. Fathpour, "Applications of thin-film lithium niobate in nonlinear integrated photonics," Adv. Photonics **4**(03), (2022).

[18] A. L. Gaeta, M. Lipson, and T. J. Kippenberg, "Photonic-chip-based frequency combs," Nat. Photonics **13**(3), 158–169 (2019).

[19] L. Chang, S. Liu, and J. E. Bowers, "Integrated optical frequency comb technologies," Nat. Photonics **16**(2), 95–108 (2022).